Mechanical and ~~Dielectric Properties~~dielectric properties of MWCNT ~~Filled Chemically Modified~~filled chemically modified SBS/PVDF ~~Blends~~blends

Christopher Ellingford

Chaoying Wan*

Chaoying.Wan@warwick.ac.uk

L. Łukasz Figiel

Tony McNally

International Institute for Nanocomposites Manufacturing (IINM), WMG, University of ~~Warwick~~Warwick, CV4 ~~7AL~~7AL, UK

*Corresponding author.

Abstract

The dielectric properties of styrene-butadiene-styrene block copolymer (SBS) were modified by two methods, covalently grafting polar methyl thioglycolate to the SBS main chains via thiol-ene click chemistry (MGSBS) and fabrication of nanocomposites by melt-blending with poly(vinylidene fluoride) (PVDF) and multi-walled carbon nanotubes (MWCNTs). The methyl thioglycolate pendant groups enhanced the dielectric permittivity of SBS from 4.4 to 11.8 at 1 kHz, ascribed to the increased dipole content of the SBS matrix under the applied electric field. The subsequent modification of MGSBS:PVDF:MWCNT composites at (69.5:29.5:1) wt% showed a maximum dielectric permittivity of 24.3 at 1 kHz along with a lower tensile strength and a higher elongation at break compared to their unmodified SBS counterpart composites. This can be ascribed to the enhanced compatibility between the MGSBS and PVDF as well as the increased electrical conductivity achieved by addition of MWCNTs. This work indicates that the increase of the SBS polarity by chemical modification is an effective way to enhance the dielectric and mechanical performance of the elastomeric nanocomposites.

Keywords: Dielectric ~~Elastomer~~elastomer; Nanocomposite; Chemical ~~Modification~~modification

1 Introduction

Dielectric elastomers have been the focus of intense research interest due to key characteristics that they possess, namely, high energy densities, flexibility, whilst simultaneously being cheap, lightweight and chemically ~~stable.~~stable [1–5]. As a class of electroactive polymers, dielectric elastomers have been widely investigated as advanced materials for actuators and energy ~~harvesters.~~harvesters [6].

The dielectric permittivity (ε) of dielectric elastomers such as poly(dimethylsiloxane)-(PDMS) [7] and styrene-butadiene-styrene (SBS) [8] is typically between ~~2–3,~~2 and 3, semi-crystalline poly(vinylidene fluoride)-(PVDF) has an ε of ~~12.~~12 [9]. These are generally much lower than piezoelectric ceramic materials, such as lead zirconium titanate (PZT, ~~ε ~ 1300)~~ ε ~ 1300) and barium titanate ($BaTiO_3$, ~~ε ~ 1700).~~ε ~ 1700) [10]. For dielectric capacitor applications, the elastomers should have higher ε values in order to store greater amounts of charge and harvest more energy.

To enhance the dielectric properties of elastomers, three methodologies are generally applied: (1) blending with PVDF or its analogous structures, (2) adding electrically conducting (e.g. carbon nanotubes (CNTs)) or dielectric ceramic (e.g. $BaTiO_3$) fillers, and (3) increasing the polarity of the polymer chains by introducing electric dipoles.

For example, blending PVDF with the terpolymer, poly(vinylidene fluoride-trifluoroethylene-chlorofluoroethylene)-P(VDF-TFE-CFE) resulted in an enhanced ε up to 50 at 1 kHz, alongside a high electrical breakdown strength of 500 V μm^{-1} and an energy density of 19.6 J cm^{-3} [11].

Addition of conducting fillers in small quantities (less than a few wt%) to the polymer matrix can simultaneously enhance both electrical and mechanical properties. This has been well utilised for both PDMS and PVDF where ε were reported up to 89.5 and 225 when incorporating thermally expanded graphene nanoplatelets (Tr-GNP) and partially reduced graphene oxide (rGO), ~~respectively.~~respectively [12,13]. However, addition of electrically conducting fillers can also result in an increase in the dielectric loss, due to the internal conductive pathways causing leakage ~~current,~~current [14], and a reduction in the electrical breakdown strength due to enhanced local internal electric ~~fields.~~fields [15].

Silicone-based elastomers are often modified via hydrosilylation reactions. For example, with 89 mol% of grafting of allyl cyanide, ε reached 15.9, but this was at the expense of a high dielectric loss of ~~2.5.~~2.5 [7]. When grafting methyl thioglycolate to SBS via thiol-ene click chemistry, 81 mol% of grafting led to an increase in ε up to 12.2 [16] whilst grafting 100 mol% 2-(methylsulfonyl)-ethanethiol to poly(vinylmethylsiloxane) enhanced ε to ~~22.7.~~22.7 [17].

In this work, an SBS block copolymer was first grafted with methyl thioglycolate via thiol-ene click chemistry in order to increase the polarity of the polymer matrix. Subsequently, the grafted SBS copolymer was blended with PVDF and MWCNTs in order to further increase dielectric properties. The effects of chemical grafting and nanofillers addition methods were compared in order to explore the effective way towards higher performance dielectric elastomeric composite materials for energy harvesting applications.

2 Experimental

Styrene-butadiene-styrene block copolymer (SBS, Vector ~~8508~~8508A) was purchased from Dexco. Poly(vinylidene fluoride) (PVDF, Kynar 740) was purchased from Arkema. Tetrahydrofuran (THF, GPR Reactapur, 99.9%) and chloroform (GPR Reactapur, 99.9%) was from VWR, UK. Hexane (for HPLC, ~~>95%),~~ > 95%), 2,2-dimethoxy-2-phenylacetophenone (DMPA) (99%) and methyl thioglycolate (95%) were purchased from Sigma-Aldrich, UK and N,N-dimethylacetamide (99%) from Alfa Aesar, UK. Non-functionalised thin multi-walled carbon nanotubes (MWCNTs) produced by catalytic carbon vapour deposition (grade NC7000, purity > 90%) were purchased from Nanocyl S.A., Belgium. The MWCNTs had an average diameter of 9.5 nm, average length of 1.5 μm and a density of 1.85 g cm^{-3} [18].

2.1 Synthesis of methyl thioglycolate modified SBS (MGSBS)

10 g SBS was dissolved in 90 g of THF. Following this, 0.2 g of DMPA and 46.9 ml (4x molar excess relative to the butadiene block of SBS) of methyl thioglycolate was added to the solution. The solution was then irradiated with UV light ~~@ 365~~@365 nm with 25% intensity (50 W) using an OmniCure Series 2000 200 W UV lamp for 20 ~~minutes.~~min. The resulting modified SBS was purified and dried in a vacuum oven overnight at 60 °C. Mass of resulting product = 18.8 g. Grafting: 98%. ^{1}H NMR (300 MHz, $CDCl_3$): δ = 7.07 (br, ~~3~~3H, $H_{benzene}$), 6.53 (br, 2 H, $H_{benzene}$), 5.39 (br, ~~4~~4H, -HC=C**H**- and HC=C$\mathbf{H}_2$), 3.73 (S, ~~3~~3H, COOC$\mathbf{H}_3$), 3.23 (S, ~~2~~2H, OOC-C$\mathbf{H}_2$-S), 2.75 (br, ~~1~~1H, $(CH_2)_2$C**H**S), 2.64 (br, ~~2~~2H, H_2CC$\mathbf{H}_2$S), 1.73 (br, ~~2~~2H, H_2C-C$\mathbf{H}_2$-CH), 1.55 (br, ~~6~~6H, $(-H_2C)_2C\mathbf{H}_2$, -HCC$\mathbf{H}_2CH_2$- and $(-HC)_2CH_2$), 1.43 (br, ~~2~~2H, -HCC$\mathbf{H}_2CH_2$), 1.26 (br, ~~1~~1H, $(H_2C)_3$C**H**) ppm. FT-IR (cm^{-1}): 2927, 1729, 1435, 1272, 1128, 1007, 757.

2.2 Formation of SBS:PVDF and MGSBS:PVDF ~~Blends~~blends and MWCNT-containing ~~Composites~~composites

Polymer blends in the composition range between 30:70 wt% and 70:30 wt% were produced using unmodified SBS or MGSBS by melt compounding using a Haake Minilab II twin screw extruder at 225 °C and 50 rpm (parameters selected to ensure that MGSBS did not decompose in the extruder). The blends were then injection moulded in a Haake Minijet pro injection moulding machine with a cylinder temperature of 225 °C and mould temperature of 70 °C into specimens conforming to the ASTM-D638-14 type V standard. MWCNT containing composites were produced using melt compounding following the same procedure.

2.3 Characterisation

MGSBS was characterised by Fourier transform infrared spectroscopy (FT-IR) using a Bruker Tensor 27 at a resolution of 4 cm^{-1} with 32 scans ran for the background and the sample. ^{1}H NMR spectra were recorded using a Bruker Avance III HD 300 MHz spectrometer. Chemical shifts were internally referenced to TMS using $CDCl_3$. Spectra were processed using ACD/NMR processor version 12.01 (ACD/Labs). Tensile testing was performed using a Shimadzu Autograph AGS-X tester with samples and methodology conforming to ASTM-D638-14 type V. The extension rate was set to 10 mm min^{-1} (strain rate = 2.19% s^{-1}) with a 10 kN load cell at room temperature. Scanning Electron Microscopy (SEM) imaging was performed using a Carl Zeiss Sigma Field Emission SEM with samples sputter coated using an Au/Pd target. For the SBS:PVDF blends, the PVDF phase was etched using N,N-dimethylacetamide. For the MGSBS:PVDF blends, the MGSBS phase was etched using chloroform. Impedance measurements were carried out using a Princeton Applied Research Parastat MC with a PMC-2000 card and a two-point probe between ~~200 – 10~~200 and 10^6 Hz on thin films (between 100~200 μm thickness) formed by hot pressing using a Rondol manual hot press at 230 °C and 5 kN of force. Differential Scanning Calorimetry (DSC) measurements were performed using a Mettler Toledo DSC1 STAR^e between 25 °C and 220 °C at a heating and cooling rate of 20 °C min^{-1} for two cycles. Gel Permeation Chromatography (GPC) was carried out using an Agilent 390-MDS with 2 PLgel Mixed-C columns and THF with 2% TEA + 0.01% BHT as eluent and analysed using Agilent GPC/SEC software.

3 Results and discussion

3.1 Synthesis of methyl thioglycolate modified SBS (MGSBS)

MGSBS was synthesised with a methyl thioglycolate molar concentration of 4:1 relative to the butadiene block of SBS. The thiol concentration affects the thiol-ene click reactions. Gelation has been reported in other thiol-ene click reactions of SBS at excess thiol concentrations, and the thiol:butadiene ratio was therefore kept above 5:1 to avoid crosslinking (gelation) of ~~chains.~~chains [19]. In our case, the methyl thioglycolate:butadiene molar ratio could be reduced to 3:1 and the reactions were performed in open air and at ambient conditions. The chemical structures of the resultant MGSBS were analysed with ^{1}H NMR and FT-IR. As shown in Fig. 1A, the characteristic peaks of CH_3 and

CH_2 from methyl thioglycolate clearly appear at 3.73 and 3.23 ppm respectively in MGSBS, accompanied by the reduced intensity of alkene peaks of butadiene at 5.39 and 4.98 ppm, indicating the reaction between the alkene groups and methyl thiol(should read 'thioglycolate' not 'thiolglycolate' as seen elsewhere in the document)glycolate has taken place. FT-IR confirmed the presence of a C=O stretch from an ester group at 1729 cm^{-1} and two C-O stretches at 1272 and 1128 cm^{-1}, suggesting the successful grafting of methyl thioglycolate to SBS. The grafting efficiency is calculated from ^1H NMR to be 98 mol% with respect to the butadiene section.

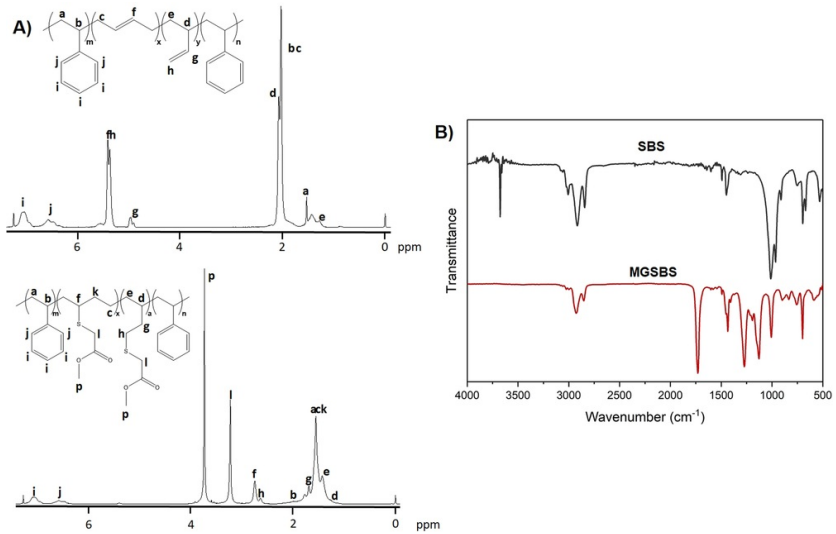

Fig. 1 A) Assigned ^1H NMR and B) FT-IR spectra for SBS and MGSBS.

alt-text: Fig. 1

By grafting methyl thioglycolate to SBS, some of the chains were damaged through scission, as shown by the reduction in number average molecular weight (M_n) and increase in polydispersity index (PDI), see Table 1. The large increase in the weight average molecular weight (M_w) further confirmed the high grafting of methyl thiol(should read 'thioglycolate' not 'thiolglycolate' as seen elsewhere in the document)glycolate to SBS.

Table 1 GPC measurement of SBS and MGSBS.

alt-text: Table 1

Polymer	M_n [g mol^{-1}] ~~n -1~~	M_w [g mol^{-1}] ~~w -1~~	PDI
SBS	86,158	100,768	1.17
MGSBS	79,417	203,883	2.57

3.2 Electrical ~~Properties~~properties of SBS:PVDF and MGSBS:PVDF ~~Blends~~blends

The dielectric permittivity (ε), tan δ, where tan δ = $\frac{dielectric\ loss}{dielectric\ permittivity}$ and AC conductivity were recorded with impedance spectroscopy, shown in Fig. 2. The MGSBS has a higher ε of 11.8 as compared to unmodified SBS of 4.4.

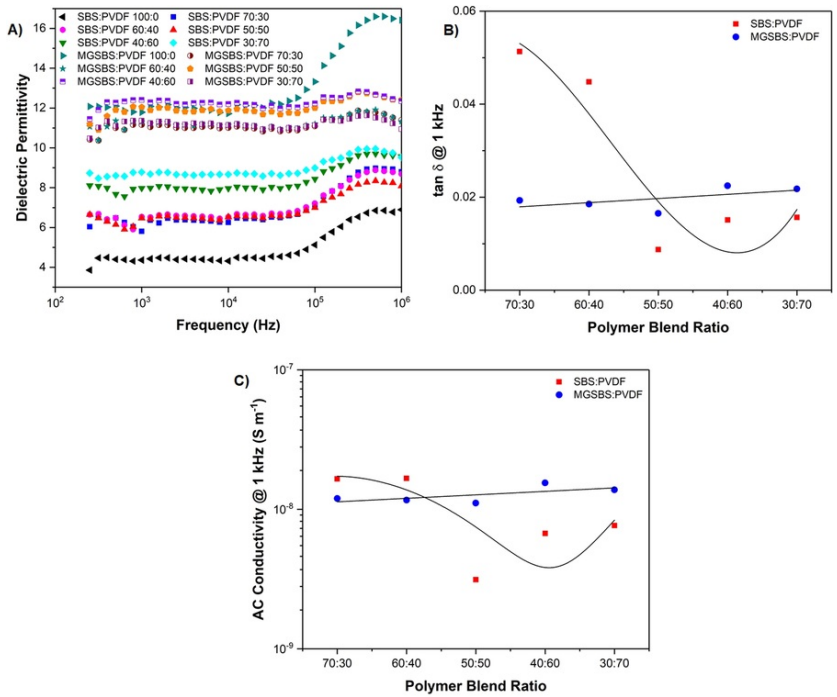

Fig. 2 Changes in A) average dielectric permittivity, B) average tan δ and C) average AC conductivity of SBS:PVDF and MGSBS:PVDF blends as a function of frequency. Trend lines for guiding only.

alt-text: Fig. 2

The ε of the SBS:PVDF blends increased from 5.8 for 70:30 wt% to 8.8 for 30:70 wt% at 1 kHz. Whereas the blending of MGSBS with PVDF had minimal impact on the ε due to the similar ε values between MGSBS and PVDF (ε is 12). This shows that the blend ratios can be tuned between the two polymers, to alter the mechanical properties for different applications with no effect on dielectric properties.

Likewise, tan δ for the polymer blends at 1 kHz are similar to one another with all samples between 0.01 and 0.06 regardless of using SBS or MGSBS. This shows that the chemical modification and blending of polymers has a minimal effect on the losses exhibited by the system.

The AC conductivity of all the blends typically remained within an order of magnitude of each other at 1 kHz. The AC conductivity for MGSBS:PVDF blends does not vary, whereas for SBS:PVDF blends a 50 wt% content of PVDF or higher resulted in a relatively large drop in AC conductivity compared to the other SBS:PVDF blends. This suggests a change in the morphology of the blend arose resulting in a poorer conductive pathway in the matrix.

3.3 Mechanical ~~Properties~~properties

The mechanical properties of the SBS:PVDF and MGSBS:PVDF blends depend on the PVDF concentration. For the SBS:PVDF blends, an increase in PVDF concentration leads to increased tensile strength and Young's modulus, see Fig. S2~~Figure S2,~~ due to the rigidity of the semi-crystalline PVDF compared to SBS. Whilst for MGSBS:PVDF blends, the tensile strength drops considerably relative to the SBS:PVDF blends, but the elongation at break of all the samples was significantly enhanced.

Specifically, a drop was observed in the Young's modulus from 163.1 MPa at 30:70 wt% to 15.6 MPa at 70:30 wt% for MGSBS:PVDF. The largest value for the elongation at break for SBS:PVDF blends occurred for 70:30 wt% at 93%. In comparison, the greatest elongation at break for MGSBS:PVDF samples was 267% for the 60:40 wt% blend. The elongation at break was 120% lower for the 70:30 MGSBS:PVDF blend, attributed to the larger amount of damaged MGSBS chains, as a consequence of the grafting reaction, in the blend causing the failure.

The reduced mechanical properties of MGSBS and the subsequent blends with PVDF can be explained by the presence of the methyl thioglycolate pendant groups, which introduces better phase mixing between the styrene and butadiene sections of the polymer [16], leading to a reduction in strength but an increase in the maximum strain of the material. When blended with PVDF, the ester groups of MGSBS increase the interactions with ~~fluoro-~~

~~groups~~ fluoro-groups of PVDF, thus enhancing compatibility between both, which was further confirmed by examining the phase morphology of the blends by SEM, Fig. 3, and from FT-IR spectra, Fig. 4.

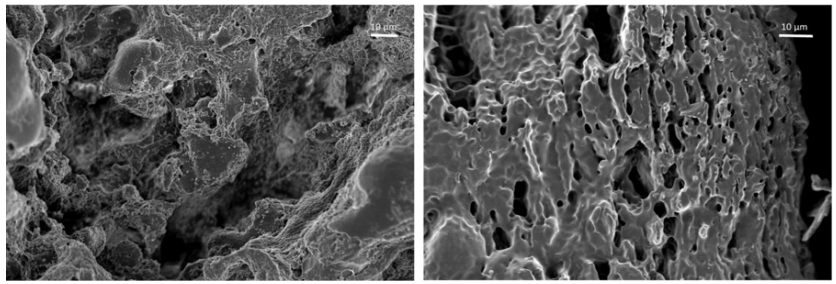

Fig. 3 SEM images of SBS:PVDF 50:50 (left) and MGSBS:PVDF 50:50 (right).

alt-text: Fig. 3

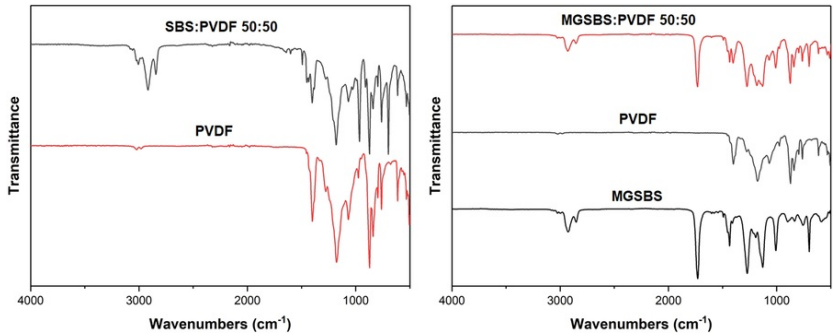

Fig. 4 Stacked normalised FT-IR Spectra of PVDF, MGSBS, SBS:PVDF 50:50 and MGSBS:PVDF 50:50.

alt-text: Fig. 4

Fig. 3 shows the phase morphology of SBS:PVDF 50:50 and MGSBS:PVDF 50:50 where the PVDF phase in SBS:PVDF and the MGSBS phase in MGSBS:PVDF were removed. The reduced phase dimension in MGSBS:PVDF and the smaller voids observed inside the PVDF phase as compared to that of SBS:PVDF demonstrate an improved compatibility and a strong interaction between PVDF and MGSBS.

The summary of key FT-IR transmission peaks from Fig. 4 are listed in Table S1~~Table S1.~~ . This shows that upon blending SBS with PVDF, there is no change in intensity between the two C-F stretches for PVDF, indicating that there is little interaction between the two phases. However, there is a change in intensity for both C-F and the ester peaks in MGSBS:PVDF 50:50 (normalised to C-H stretch at 2917 cm^{-1}). In MGSBS:PVDF 50:50, the C=O stretch at 1732 cm^{-1} and the C-O stretch at 1272 cm^{-1} reduce to the same intensity as the C-O stretch at 1130 cm^{-1} upon blending with PVDF compared to the peak intensities for MGSBS. The ratio between the two C-F stretches intensifies in MGSBS:PVDF 50:50 compared to the C-F stretches for neat PVDF. This shows that there is an increased interaction between MGSBS and PVDF compared to SBS and PVDF.

After addition of 1 wt% of MWCNTs to both SBS:PVDF 50:50 and MGSBS:PVDF 50:50 blends, a reduction in tensile strength was observed for SBS:PVDF:MWCNT (49.5:49.5:1) from 17.7 to 14.1 MPa, as seen in Fig. 5. In comparison, addition of MWCNTs demonstrated effective reinforcement effects for MGSBS:PVDF:MWCNT (49.5:49.5:1) whereby the tensile strength was increased from 3.92 to 7.90 MPa. Similarly, the addition of MWCNTs reduced the Young's modulus of SBS:PVDF:MWCNT (49.5:49.5:1), i.e. a reduction from 472 to 337 MPa was attained, but for MGSBS:PVDF:MWCNT (49.5:49.5:1), an increase from 33 to 93 MPa was obtained. As a result, the elongation at break for MGSBS:PVDF:MWCNT (49.5:49.5:1) decreased from 67% to 44%, whilst little effect on the extensibility of SBS:PVDF:MWCNT (49.5:49.5:1) was observed.

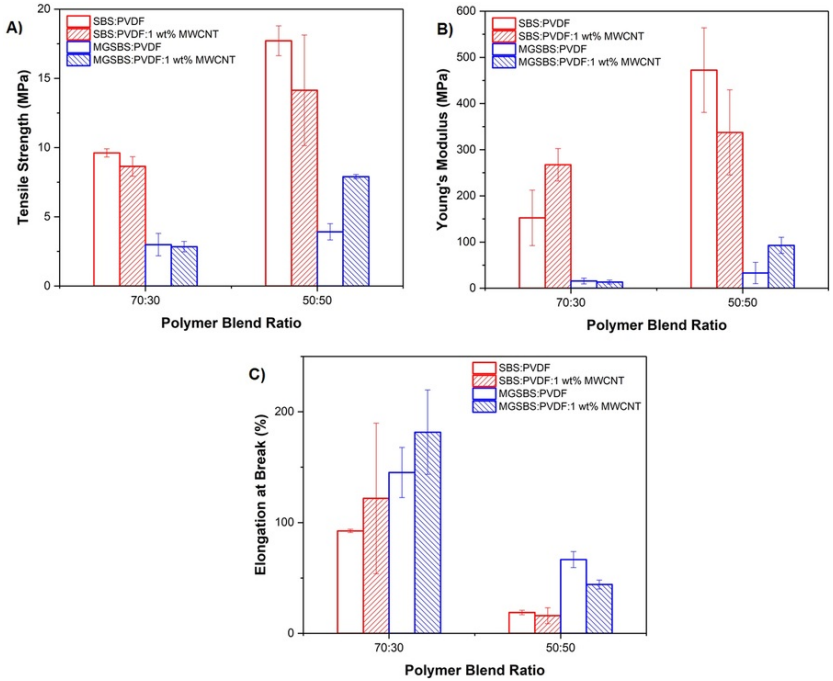

Fig. 5 Changes in A) tensile strength, B) Young's modulus and C) elongation at break of SBS:PVDF:MWCNT and MGSBS:PVDF:MWCNT samples as a function of blend ratio.

alt-text: Fig. 5

When MWCNTs were added to SBS:PVDF 70:30 and MGSBS:PVDF 70:30, the tensile strength remained similar for SBS:PVDF:MWCNT (69.5:29.5:1). In comparison, addition of MWCNTs also had little effect on the tensile strength of MGSBS:PVDF:MWCNT (69.5:29.5:1). The Young's modulus increased from 152 to 267 MPa for SBS:PVDF:MWCNT (69.5:29.5:1) but for MGSBS:PVDF:MWCNT (69.5:29.5:1) there was no effect. However, elongation at break increased for both composites, from 93% to 122% and 145 to 182% for SBS:PVDF:MWCNT (69.5:29.5:1) and MGSBS:PVDF:MWCNT (69.5:29.5:1), respectively.

Table S2 shows the percentage crystallinity, X_c(%), crystallisation temperature (T_c) and melting temperature (T_m) of the PVDF phase of the composites from DSC. Both T_c and T_m of the PVDF phase remain constant regardless of the sample tested. However, the X_c changed significantly between samples depending on how the X_c of the PVDF phase was affected. By blending MGSBS with PVDF, X_c of the samples decreased by up to 14% compared to neat PVDF, possibly due to the enhanced compatibility between the two phases. Addition of MWCNTs to SBS:PVDF, the MWCNTs lowered the X_c by up to 2.7%. After addition of the MWCNTs, X_c then returned to a value close to that of PVDF, due to the MWCNTs providing heterogeneous nucleation sites for ~~crystallisation.~~crystallisation [20].

SEM images were taken of the SBS:PVDF:MWCNT and MGSBS:PVDF:MWCNT samples. From Fig. 6A, the image shows the SBS phase of SBS:PVDF:MWCNT (49.5:49.5:1) with a number of white dots throughout the image, attributed to the MWCNTs. Fig. 6B shows the PVDF phase of MGSBS:PVDF:MWCNT (49.5:49.5:1) blends and shows reduced phase dimensions and a large number of white dots ascribed to the charging of the ends of MWCNTs under the electron beam.

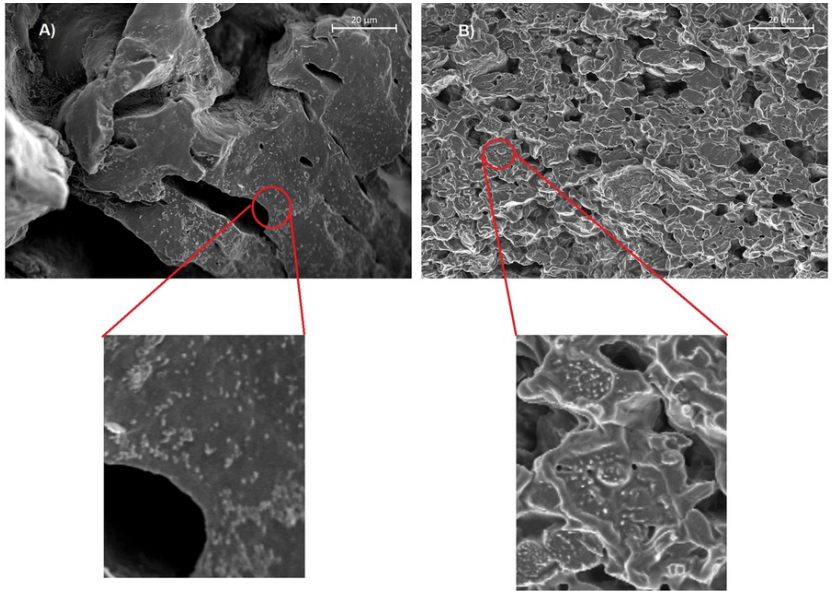

Fig. 6 SEM images of A) the SBS phase in SBS:PVDF:MWCNT and B) the PVDF phase in MGSBS:PVDF:MWCNT with a zoomed in section of the image.

alt-text: Fig. 6

Firstly, for the composites containing MGSBS a reinforcement or minimal reduction of the mechanical properties was observed. This suggests that it is easier to achieve a good dispersion of MWCNTs throughout the polymer matrix when MGSBS was used for blending with PVDF compared to SBS, confirmed from the reduced phase dimensions observed in the SEM images for the nanocomposites.

Second, in the 50:50 MGSBS:PVDF blend, the reinforcement of the mechanical properties upon addition of MWCNTs was more pronounced compared to the 70:30 blend. The X_c of the PVDF phase in MGSBS:PVDF:MWCNT (49.5:49.5:1) was similar to the X_c of neat PVDF and was matched by an increase in stress and a reduction in the ductility of the composite. Therefore, introduction of MWCNTs into MGSBS:PVDF 50:50 enhanced X_c of PVDF by providing nucleation sites for crystalline regions to form [20] and a mechanical reinforcement was observed. This suggests that the blends containing a greater quantity of PVDF are able to disperse MWCNTs much more readily, implying that the MWCNTs preferentially locate in the PVDF phase of the blend compared to the MGSBS phase.

By comparison, the SBS:PVDF:MWCNT systems exhibit a reduction in strength for both the 70:30 and 50:50 blends. The X_c for SBS:PVDF 50:50 was higher SBS:PVDF 70:30 due to the larger PVDF phase content promoting crystallisation of PVDF. However, upon addition of MWCNTs, X_c of PVDF for both composites decreased. The decrease in mechanical properties is attributed to a poorer dispersion of MWCNTs disrupting the polymer matrix.

SBS is more compatible with MWCNTs than MGSBS, and the SEM images show a number of MWCNTs present in the SBS phase. As both polymers are able to interact with the MWCNTs, the crystallinity of PVDF was reduced. The ability of SBS to interact with MWCNTs is explained by π-π stacking through the styrene ~~groups,~~groups [21], which is allowed by the predominately-linear butadiene section of the block copolymer.

By modification of SBS with methyl thioglycolate, the ester groups prevent π-π stacking, by altering the packing of the MGSBS chains through increased phase mixing between the styrene and butadiene blocks, compared to SBS ~~chains.~~chains [16]. Without sufficient π-π stacking and a greater compatibility between MGSBS and PVDF, the MWCNTs will preferentially locate in the PVDF phase.

3.4 Electrical ~~Properties~~properties of the SBS:PVDF:MWCNT and MGSBS:PVDF:MWCNT ~~Composites~~composites

The effect of MWCNTs on the ε, tan δ and AC conductivity was then investigated, see Fig. 7. The maximum ε for the SBS composites was 11.7 at 1 kHz for (49.5:49.5:1). In comparison, MGSBS:PVDF:MWCNT containing (49.5:49.5:1) and (69.5:29.5:1) exhibited ε of 16.3 and 24.3 respectively, at 1 kHz, showing a marked improvement.

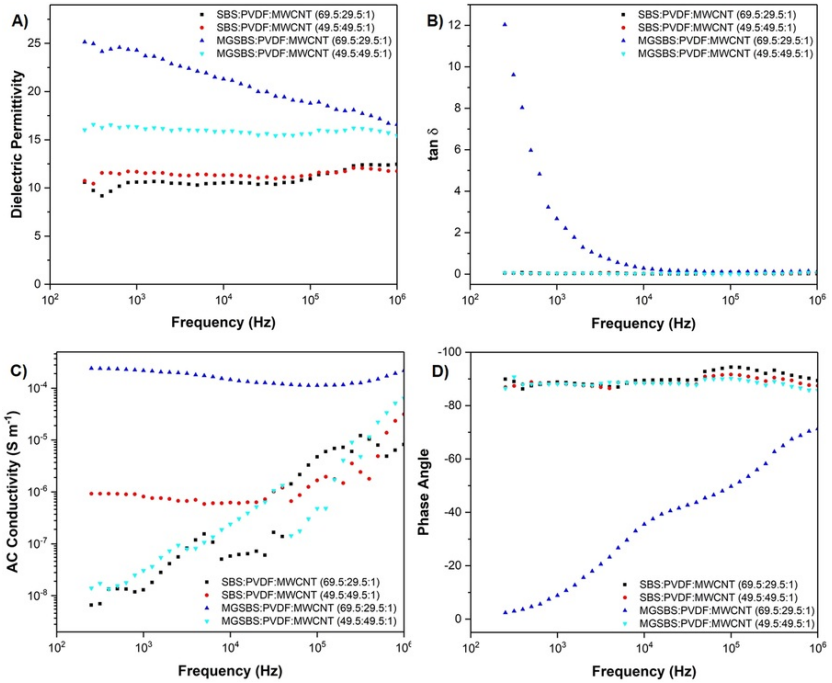

Fig. 7 Changes in A) average dielectric permittivity, B) average tan δ, C) average AC conductivity and D) average phase angle of SBS:PVDF:MWCNT and MGSBS:PVDF:MWCNT nanocomposites as a function of frequency.

alt-text: Fig. 7

The AC conductivity of MGSBS:PVDF:MWCNT (69.5:29.5:1) remained constant at 10^{-4} S m^{-1}, independent of the applied frequency, and the percolation threshold was reached. The tan δ was high, reflecting the formation of the conducting network by the ~~MWCNTs,~~MWCNTs [14], with 2.67 recorded at 1 kHz. A percolation threshold was not achieved in the (49.5:49.5:1) composite and tan δ remained low at 0.033 at 1 kHz. This reinforces the hypothesis that MWCNTs prefer to locate in the PVDF phase compared to the MGSBS phase, as with a smaller PVDF phase present a conducting network was more easily formed. As the same effect was not obtained for the SBS:PVDF:MWCNT blends, it suggests that the increase in compatibility between PVDF and MGSBS allows for the formation of a conducting network in the PVDF phase.

4 Conclusions

SBS was modified by grafting methyl thioglycolate to form MGSBS using thiol-ene click chemistry. Both SBS and MGSBS were blended with PVDF and MWCNTs in different weight ratios using melt mixing. MGSBS:PVDF blends had lower tensile strength and Young's modulus but increased elongation at break compared to the analogous SBS:PVDF blends. The ε remained constant for all the MGSBS:PVDF blends at approximately 12. Incorporation of MWCNTs into MGSBS:PVDF blends had a significant increase in electrical properties for the (69.5:29.5:1) blend where the percolation threshold was reached at 1 wt% MWCNT and the ε was measured to be 24.3 at 1 kHz. For the (49.5:49.5:1) composition, a percolation threshold was not reached and the increase in ε was to 16.3 only. This was attributed to the greater PVDF content and that the MWCNTs preferentially disperse in the PVDF phase.

Acknowledgements

CE thanks EPSRC and Jaguar Land Rover (UK) for funding hi(his should be replaced with a)s ~~PhD~~Ph.D. studentship.

Appendix A. ~~Supporting information~~Supplementary material

Supplementary data associated with this article can be found in the online version at doi:10.1016/j.coco.2017.11.001.

References

[1] J. Lee, H. Kwon, J. Seo, S. Shin, J.H. Koo, C. Pang, et al., Conductive ~~Fiber-Based Ultrasensitive Textile Pressure Sensor~~fiber-based ultrasensitive textile pressure sensor for ~~Wearable Electronics~~wearable electronics, ~~*Adv.*~~*Adv. Mater.* **27** (15), 2015, 2433–2439.

[2] M. Amjadi, A. Pichitpajongkit, S. Lee, S. Ryu and I. Park, Highly ~~Stretchable~~stretchable and ~~Sensitive Strain Sensor Based~~sensitive strain sensor based on ~~Silver Nanowire–Elastomer Nanocomposite~~silver nanowire–elastomer nanocomposite, *ACS* ~~*Nano.*~~*Nano* **8** (5), 2014, 5154–5163.

[3] R. Pelrine, R. Kornbluh, Q. Pei and J. Joseph, ~~High-Speed Electrically Actuated Elastomers~~High-speed electrically actuated elastomers with ~~Strain Greater Than~~strain greater than 100%, ~~*Science.*~~*Science* **287** (5454), 2000, 836–839.

[4] R. Shankar, T.K. Ghosh and R.J. Spontak, Electroactive ~~Nanostructured Polymers~~nanostructured polymers as ~~Tunable Actuators~~tunable actuators, ~~*Adv.*~~*Adv. Mater.* **19** (17), 2007, 2218–2223.

[5] ~~**Xuan Y, Shuai C, Gao Y, Zhao Z. Application review of dielectric electroactive polymers (DEAPs) and piezoelectric materials for vibration energy harvesting. Journal of Physics: Conference Series. 2016;744(1):012077.**~~ Y. Xuan, C. Shuai, Y. Gao and Z. Zhao, Application review of dielectric electroactive polymers (DEAPs) and piezoelectric materials for vibration energy harvesting, *J. Phys.: Conf. Ser.* **744** (1), 2016, 012077.

[6] F.B. Madsen, A.E. Daugaard, S. Hvilsted and A.L. Skov, The ~~Current State~~current state of ~~Silicone-Based Dielectric Elastomer Transducers~~silicone-based dielectric elastomer transducers, ~~*Macromol.*~~*Macromol. Rapid* ~~*Commun.*~~*Commun.* **37** (5), 2016, 378–413.

[7] C. Racles, M. Alexandru, A. Bele, V.E. Musteata, M. Cazacu and D.M. Opris, Chemical modification of polysiloxanes with polar pendant groups by co-hydrosilylation, *RSC Adv.* **4** (71), 2014, 37620–37628.

[8] M. Tian, H. Yan, H. Sun, L. Zhang and N. Ning, Largely improved electromechanical properties of thermoplastic dielectric elastomers by grafting carboxyl onto SBS through thiol-ene click chemistry, *RSC Adv.* **6** (98), 2016, 96190–96195.

[9] C. Wan and C.R. Bowen, Multiscale-structuring of polyvinylidene fluoride for energy harvesting: the impact of molecular-, micro- and macro-structure, *J* ~~*Mater Chem A.*~~*Mater. Chem. A* **5**, 2017, 3091–3128.

[10] C. Baur, D.J. Apo, D. Maurya, S. Priya and W. Voit, Advances in Piezoelectric Polymer Composites for Vibrational Energy ~~Harvesting~~Harvesting. Polymer Composites for Energy Harvesting, Conversion and Storage, ~~Polymer Composites for Energy Harvesting, Conversion and Storage~~2014, American Chemical Society, 1–27.

[11] X. Zhang, Y. Shen, Z. Shen, J. Jiang, L. Chen and C.-W. Nan, Achieving ~~High Energy Density~~high energy density in ~~PVDF-Based Polymer Blends: Suppression~~PVDF-based polymer blends: suppression of ~~Early Polarization Saturation~~early polarization saturation and ~~Enhancement~~enhancement of ~~Breakdown Strength~~breakdown strength, *ACS* ~~*Appl Mater*~~*Appl. Mater. Interfaces* **8** (40), 2016, 27236–27242.

[12] M. Tian, Z. Wei, X. Zan, L. Zhang, J. Zhang, Q. Ma, et al., Thermally expanded graphene nanoplates/polydimethylsiloxane composites with high dielectric constant, low dielectric loss and improved actuated strain, *Compos* ~~*Sci Technol*~~*Sci. Technol.* **99**, 2014, 37–44.

[13] X.-l Xu, C.-j Yang, J.-h Yang, T. Huang, N. Zhang, Y. Wang, et al., Excellent dielectric properties of poly(vinylidene fluoride) composites based on partially reduced graphene oxide, ~~*Composites,*~~*Compos. Part* ~~*B.*~~*B* **109**, 2017, 91–100.

[14] M. Li, Y. Deng, Y. Wang, Y. Zhang and J. Bai, High dielectric properties in a three-phase polymer composite induced by a parallel structure, ~~*Mater Chem Phys*~~*Mater. Chem. Phys.* **139** (2), 2013, 865–870.

[15] J.I. Roscow, C.R. Bowen and D.P. Almond, Breakdown in the ~~Case~~case for ~~Materials~~materials with ~~Giant Permittivity?~~giant permittivity?, *ACS Energy* ~~*Letters*~~*Lett.* **2** (10), 2017, 2264–2269.

[16] H. Sun, C. Jiang, N. Ning, L. Zhang, M. Tian and S. Yuan, Homogeneous dielectric elastomers with dramatically improved actuated strain by grafting dipoles onto SBS using thiol-ene click chemistry, ~~*Polym*~~*Polym. Chem* **7** (24), 2016, 4072–4080.

[17] S.J. Dunki, E. Cuervo-Reyes and D.M. Opris, A facile synthetic strategy to polysiloxanes containing sulfonyl side groups with high dielectric permittivity, ~~*Polym*~~*Polym. Chem.* **8** (4), 2017, 715–724.

[18] S.J. Chin, S. Vempati, P. Dawson, M. Knite, A. Linarts, K. Ozols, et al., Electrical conduction and rheological behaviour of composites of poly(ε-caprolactone) and MWCNTs, ~~*Polymer*~~*Polymer* **58**, 2015, 209–221.

[19] J.S. Silverstein, B.J. Casey, M.E. Natoli, B.J. Dair and P. Kofinas, Rapid ~~Modular Synthesis~~modular synthesis and ~~Processing~~processing of ~~Thiol–Ene Functionalized Styrene–Butadiene–Block Copolymers~~thiol–ene functionalized

styrene–butadiene block copolymers, ~~*Macromolecules.*~~*Macromolecules* **45** (7), 2012, 3161–3167.

[20] K. Ke, Y. Wang, K. Zhang, Y. Luo, W. Yang, B.-H. Xie, et al., Melt viscoelasticity, electrical conductivity, and crystallization of PVDF/MWCNT composites: ~~Effect~~effect of the dispersion of MWCNTs, ~~*J Appl Polym Sci*~~*J. Appl. Polym. Sci.* **125** (S1), 2012, E49–E57.

[21] T. Fujigaya and N. Nakashima, Non-covalent polymer wrapping of carbon nanotubes and the role of wrapped polymers as functional dispersants, ~~*Science and Technology of Advanced Materials*~~*Sci. Technol. Adv. Mater.* **16** (2), 2015, 024802.

Appendix A. Supplementary material

Multimedia Component 1

(In the Supplementary material document, the both figures say 'S2'. However, the first figure should be 'S1'.)Figure S1 Supplementary material

Graphical abstract

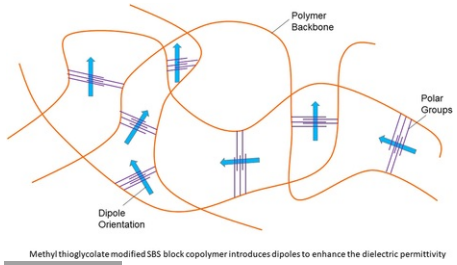

alt-text: fx1

Queries and Answers

Query:

Please confirm that given names and surnames have been identified correctly and are presented in the desired order, and please carefully verify the spelling of all authors.

Answer: The names are correct

Query:

Your article is registered as belonging to the Special Issue/Collection entitled "VSI:3rd China-UK Polymer Nanocomposites". If this is NOT correct and your article is a regular item or belongs to a different Special Issue please contact p.salma@elsevier.com immediately prior to returning your corrections.

Answer: This is correct

Query:

Please confirm if the hierarchy of section headings as edited is ok.

Answer: The hierarchy is correct

Query:

Please provide Grant number for the Grant sponsors "EPSRC" and "Jaguar Land Rover (UK)".

Answer: There is no grant number as it is a Jaguar Land Rover UK iCase sponsored Ph.D

Query:

Please provide the place of publication in Ref. [10] if available.

Answer: The place of publication is Washington (according to Web of Science)